

# Measurement of Raman-Scattering Spectra of $\text{Rb}_2\text{KMoO}_3\text{F}_3$ Crystal: Evidence for Controllable Disorder in the Lattice Structure

Published as part of the *Crystal Growth & Design* virtual special issue *Anion-Controlled New Inorganic Materials*.

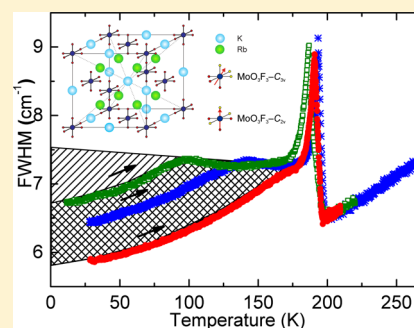
A. S. Krylov,<sup>\*,†</sup> E. M. Kolesnikova,<sup>†</sup> L. I. Isaenko,<sup>‡</sup> S. N. Krylova,<sup>†</sup> and A. N. Vtyurin<sup>†</sup>

<sup>†</sup>L. V. Kirensky Institute of Physics, SB RAS, 660036, Krasnoyarsk, Russia

<sup>‡</sup>V. S. Sobolev Institute of Geology and Mineralogy, SB RAS, 630090, Novosibirsk, Russia

**W** Web-Enhanced Feature

**ABSTRACT:** The  $\lambda$ -shaped line width broadening anomalies of octahedron group vibrations in  $\text{Rb}_2\text{KMoO}_3\text{F}_3$  disordered crystal have been revealed in the wide temperature range by Raman technique. The line width of Mo–O and Mo–F vibrations in this crystal is connected with the lattice disorder. The dependence of ordering degree passing the phase transition point history has been discovered. Wide temperature–line width area is found below structural phase transition where different lattice disorder can be obtained at a given temperature by varying the rate of sample cooling. The current study demonstrates the ability of a dynamic temperature regime to control ordering processes in crystals.



Elpasolite,  $\text{Rb}_2\text{KMoO}_3\text{F}_3$ , as well as other oxyfluoride compounds with general formula  $\text{A}_2\text{BMeO}_x\text{F}_{6-x}$  ( $x = 1$  or  $3$ ), belongs to a family with cubic symmetry in its high temperature phase. However, due to the presence of two types of anions (F and O) in the anionic octahedra, their local symmetry is less than cubic, and it can be either  $C_{3v}$  or  $C_{2v}$ , depending on the relative positions of F and O anions corresponding to *fac*- or *mer*-isomers, respectively, see Figure 1.

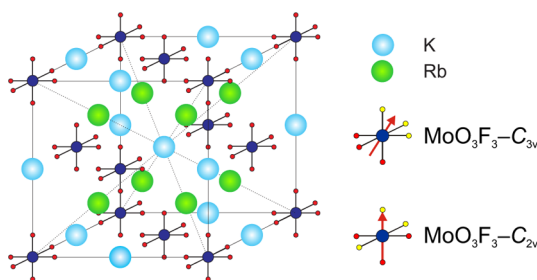


**Figure 1.** Structure of  $\text{Rb}_2\text{KMoO}_3\text{F}_3$  in the cubic  $Fm\bar{3}m$  phase. Red arrows show dipole moment directions of quasi-octahedra.

Owing to the difference in partial electron charges of two anions, F and O, both isomers possess dipole moments. At the same time, the space symmetry group of oxyfluoride compounds remains  $Fm\bar{3}m$  ( $Z = 4$ ) due to disordering of F and O positions and, consequently, disordering of the octahedra in the crystal lattice.<sup>1</sup> Upon cooling, after passing the phase transition temperature, the crystal symmetry is reduced and disorder in the structure is decreased in whole or

in part. This is the case for all crystals of the family; the disorder degree is independent of cooling history, and it is the same in all experiments. Detailed explanation of structure and structural properties can be found in ref 2. Of significant interest in oxyfluorides is to find compounds that have an intrinsic dipole moment and at the same time could exhibit an induced dipole moment either under external fields or due to structural phase transitions. Compounds with such properties have been extensively utilized in numerous practical applications, and they are subject to worldwide studies by many research groups.<sup>3–9</sup>

Earlier studies demonstrate that elpasolite,  $\text{Rb}_2\text{KMoO}_3\text{F}_3$ , undergoes two subsequent phase transitions, one at  $T = 328$  K (accompanied by spontaneous polarization) and the other at  $T = 182$  K.<sup>10–14</sup> However, more recent investigations of numerous samples synthesized by different methods reveal only order–disorder phase transition at  $T = 195$  K;<sup>9</sup> this transition is further characterized to be ferroelastic and far from the tricritical point.

Recent investigations of the crystal lattice dynamics for  $\text{Rb}_2\text{KMoO}_3\text{F}_3$  were carried out using Raman technique.<sup>15</sup> Order–disorder phase transition was observed during sample cooling at temperature  $T \approx 185$  K. This transition is further characterized to be ferroelastic and far from the tricritical point. The structure of the low temperature phase remains unknown.<sup>9</sup> The observed line width anomalies are indicative of the phase

**Received:** June 29, 2013

**Revised:** December 11, 2013

**Published:** January 20, 2014

transition since, according to ref 16, the widths of stretching vibrations, such as those of Mo–O and Mo–F, are strongly correlated with the degree of crystal ordering. Also Raman and X-ray studies indicated that  $[\text{MoO}_3\text{F}_3]^{3-}$  octahedra have mostly *fac*-configuration.<sup>3,17</sup>

The aim of this study is to clarify the nature of line width anomalies in the low temperature phase of  $\text{Rb}_2\text{KMoO}_3\text{F}_3$  as well as the mechanism of structure ordering using Raman technique, combining high spectral resolution and small temperature increments to obtain as detailed data as possible.

Raman spectra of single crystals  $\text{Rb}_2\text{KMoO}_3\text{F}_3$  were taken by a Horiba Jobin Yvon T64000 spectrometer using LN cooled CCD detector. The spectrometer was adjusted to an additive dispersion mode with the spectral resolution  $0.7\text{ cm}^{-1}$ , a pixel covering  $0.1\text{ cm}^{-1}$  of the spectral range. We used sample 7 described in ref 9. Sample size was about  $1.5 \times 1.5 \times 1.5\text{ mm}^3$ , with no impurities visible under the microscope. The low temperature experiments were carried out using a closed cycle helium cryostat ARS CS204-X1.SS, controlled by a LakeShore 340 temperature controller. The temperature was monitored by a calibrated silicon diode, LakeShore DT-670SD1.4L. The precision of sample temperature stabilization for each cooling rate is given in Table 1. Indium foil was used as a thermal

**Table 1. Precision of Cooling Rate vs Temperature Stabilization**

cooling rate (K/min)	precision of temperature stabilization (K)
7.0	$\pm 0.58$
5.0	$\pm 0.42$
3.0	$\pm 0.25$
1.5	$\pm 0.35$
1.0	$\pm 0.25$
0.7	$\pm 0.18$
0.5	$\pm 0.13$
0.2	$\pm 0.05$

interface. Measurements were taken inside the cryostat under pressure of  $10^{-6}$  mbar. An  $\text{Ar}^+$  ion laser with  $\lambda = 514.5\text{ nm}$  and power = 7 mW on a sample was used as an excitation light source. The above instrumentation allows one to vary the sample cooling rate from 0.2 to 15 K/min with 0.1 K/min intervals.

The experiments were carried out in the dynamic regime by varying the sample temperature. The rates of temperature variation ranged from 0.1 to 7 K/min in different experiments. The uncertainty of the measured temperature for a given rate can be estimated as a difference between adjacent measurements. Overall time for a single spectrum accumulation was within 30 s. The spectra were acquired with a temperature step from 0.2 to 0.25 K.

To obtain quantitative information, the spectra were deconvoluted into separate spectral lines. To describe lines shape we used the Lorentz function:

$$I(\omega) = \frac{2}{\pi} \frac{A\Gamma}{4(\omega - \omega_0)^2 + \Gamma^2} \quad (1)$$

where  $A$ ,  $\omega_0$ ,  $\omega$ , and  $\Gamma$  are the amplitude, position of the line center, wavenumber, and full width at half-maximum (fwhm), respectively. The explanation of analysis is similar to that given in ref 18.

The effect of anomalous line broadening for stretching vibrations of Mo–O and Mo–F is described in ref 15. Note

that Mo–O stretching is the most intensive line in the spectra. Therefore, the spectral parameters of this line can be obtained quite accurately. In our work, we obtain line position by peak fitting using all points of spectral shape. In our case, this was more than 150 points per spectral shape on average. Therefore, this can give us about 12 times better results than coverage of a single CCD pixel. In the above experiments, the uncertainty in the line width is estimated to be within  $0.03\text{ cm}^{-1}$  (for evidence of this estimate we carried out measurements for a series of 100 spectra in the temperature stabilization regime). As a result, one can easily distinguish small changes (about  $0.5\text{ cm}^{-1}$ ), since this is an order of magnitude larger than the uncertainty of the above measurements.

The experimental wavenumbers are found to be in good agreement with those estimated in quantum-chemical calculations of the  $[\text{WO}_3\text{F}_3]^{3-}$  octahedron dynamics as described in ref 17. Due to isostructurality, the shape of the Raman spectra of  $[\text{MoO}_3\text{F}_3]^{3-}$  octahedra in the  $\text{Rb}_2\text{KMoO}_3\text{F}_3$  crystal is identical to the shape of the Raman spectra of  $[\text{WO}_3\text{F}_3]^{3-}$ , the only difference being a minor shift in absolute positions of the spectral lines. Based on this observation, one can assign the spectral lines at 904 and  $359\text{ cm}^{-1}$  to fully symmetric Mo–O and Mo–F stretching vibrations, respectively.

In ref 15, a part of the spectra containing the Mo–O vibration line is recorded with  $2\text{ cm}^{-1}$  spectral resolution, and in the high temperature phase, this line is fitted to a single Lorentzian contour; due to the large difference between model simulations and experimental data, it seems pointless to deconvolute these experimental spectra into several Lorentzians. However, in the current study, this part of the spectra has a much better spectral resolution ( $0.7\text{ cm}^{-1}$ ), allowing one to study this spectral contour more carefully. The analysis of the spectra shows their reproducible asymmetry, which indicates the presence of at least two spectral lines within the contour (Figure 2b) even though this Mo–O stretching in the cubic

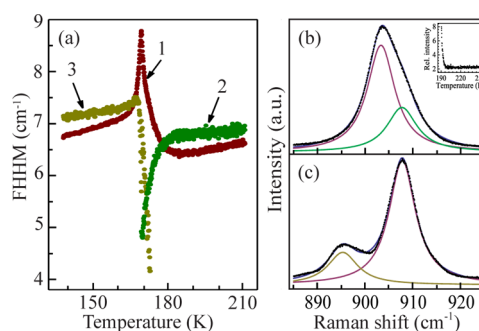


**Figure 2.** (a) Temperature dependence of the line width in the range of the Mo–O stretching vibration (1,  $904\text{ cm}^{-1}$ ; 2,  $908\text{ cm}^{-1}$ ; 3,  $895\text{ cm}^{-1}$ ). Transformation of the Raman spectrum in the range of stretching vibration MoO: (b) before phase transition at  $T = 220\text{ K}$  and (c) after phase transition at  $T = 100\text{ K}$ . The inset shows the dependence of the relative intensity  $I_{904\text{cm}^{-1}}/I_{908\text{cm}^{-1}}$  in the cubic phase.

phase is nondegenerate. The temperature dependence of the intensity ratio of the two lines in the cubic phase is shown in the inset of Figure 2b.

The transition to the low-temperature phase is accompanied by the symmetry change and, consequently, by a  $895\text{ cm}^{-1}$  line appearing in the spectrum. Therefore, in this paper, the phase transition temperature is determined by the appearance of the  $895\text{ cm}^{-1}$  line, see Figure 2a.

At  $T = 195$  K, which is the phase transition temperature in the heating regime,<sup>9</sup> there are three lines in the spectral region corresponding to the Mo–O vibration: 895, 904, and 908  $\text{cm}^{-1}$ . Spectra transformation is given in Figure 3 and in a

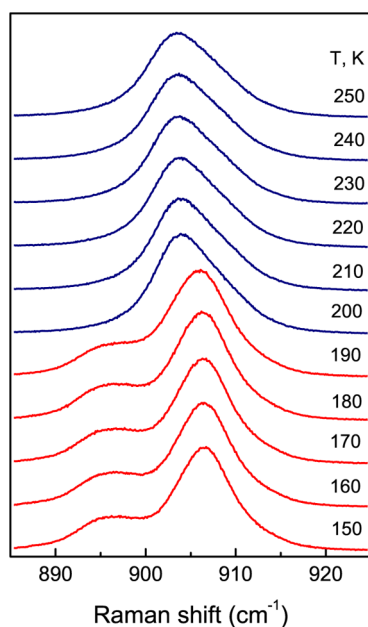


**Figure 3.** Temperature spectra transformation at the region of Mo–O stretching vibration in heating regime with heating rate 0.5 K/min.

supplementary movie. The lines can be observed all together only in a narrow temperature range,  $\Delta T$  of about 5 K, below the phase transition temperature. At lower temperatures, spectra contain only two lines at 895 and 904  $\text{cm}^{-1}$ , while at higher temperatures there are two lines at 904 and 908  $\text{cm}^{-1}$ . As seen in the inset of Figure 2b, the intensity of the 908  $\text{cm}^{-1}$  line reduces to zero below the phase transition, while another spectral line at 904  $\text{cm}^{-1}$  splits into two (Figure 2c).

The experimental intensity ratio of these two lines,  $I_{904\text{cm}^{-1}}/I_{908\text{cm}^{-1}}$ , is found to be nearly constant and equal to 2 in the entire temperature range above the transition point. Note that two lines are also observed in the region of fully symmetric Mo–F stretching vibrations.

It is known that the widths of the fully symmetric vibrations of an anionic octahedron in ordered elpasolite compounds under liquid helium temperature are about 1–3  $\text{cm}^{-1}$ .<sup>19–21</sup> The fully symmetric vibration at 904  $\text{cm}^{-1}$  is present in all phases of the compound under investigation; therefore, the width of this line as a temperature function could be a useful indicator of the ordering degree of  $[\text{MoO}_3\text{F}_3]^{3-}$  octahedra. It has been found that even under helium temperature the width of Mo–O vibrations in the given sample is several times larger than that expected for fully ordered elpasolites, indicating that these groups are not fully ordered even at these temperatures.

The temperature dependence of the Mo–O vibration line width is shown in Figure 2a. One can clearly see an anomalous  $\lambda$ -shaped spike at the transition temperature. The presence of such a spike in the width vs temperature dependence is quite unusual for crystals; it is much more common to see such spikes during gas to liquid phase transitions.<sup>22,23</sup> Such peculiar behavior of the line width is believed to be due to a structure ordering near the phase transition point in order–disorder phase transitions.<sup>24,25</sup>

The line width behavior shown in Figure 4a,b indicates that processes connected with the phase transition are spread over

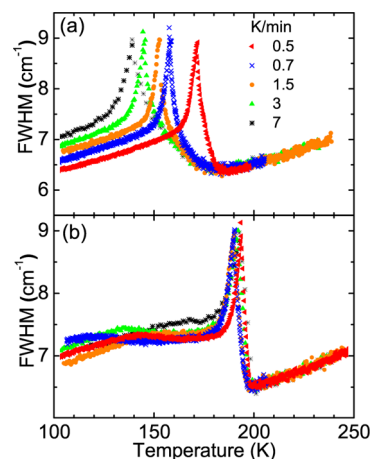


**Figure 4.** Temperature dependences of the line width of Mo–O stretching vibration at different cooling (a) and heating rates (b).

about 20 K in the cooling regime and over about 15 K in the heating regime. At temperatures near the phase transition region, the line width increases sharply at first and then decreases. In the low temperature phase, the line is wider, indicating that the anionic octahedra are more disordered in this phase compared with the cubic one. The experimental data also reveals strong variations of the transition region as a function of cooling/heating rate. For example, in the cooling regime, Figure 4a, this range varies from 20 K (cooling rate of 0.5 K/min) to 65 K (cooling rate of 7 K/min). In the heating regime, Figure 4b, it varies from 15 K (heating rate of 0.5 K/min) to 18 K (heating rate of 7 K/min). Despite spreading phase transition, the temperature when the 895  $\text{cm}^{-1}$  line appears in the spectrum changes insignificantly. This is consistent with the results of the calorimetric investigations.<sup>9</sup>

The temperature hysteresis of this phase transition is about 15 K as seen in Figure 5. Normally for the crystals with

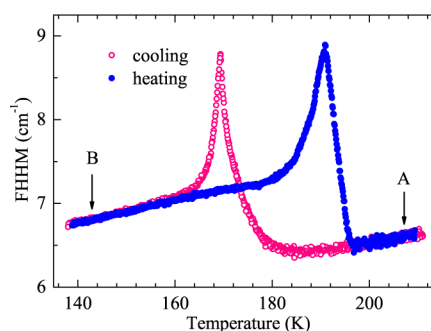


**Figure 5.** Phase transition hysteresis of the line width of the Mo–O stretching vibration (cooling and heating rates, 0.2 K/min).

hysteresis far away from the transition where heating and cooling curves overlap (e.g., points A and B in Figure 6), spectral parameters are independent of the previous experimental procedure. Indeed, such behavior has been observed in the given study for the cubic phase and in the quasistatic temperature regime (Figure 5). However, below the phase transition point in the low temperature phase one should note

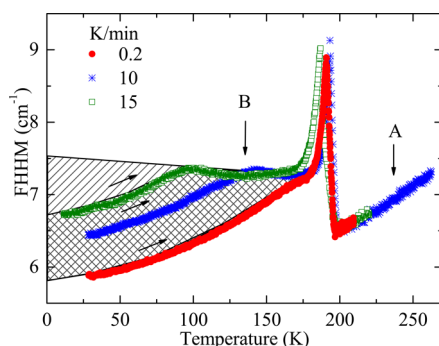


**Figure 6.** Temperature dependences of the line width of Mo–O stretching vibration with heating rate 0.5 K/min after cooling at different rates. Double shading denotes the experimentally obtained controllable area with maximum cooling rate 15 K/min, and single shading shows estimated area with cooling rate of about 30 K/min.

the dependence of the line width on the cooling rate in the vicinity of the phase transition, see point B in Figure 6.

Depending on the cooling rate, different line widths are observed at 10 K, the width varying from 5.7 to 6.7  $\text{cm}^{-1}$  for cooling rates of 0.2 and 15 K/min, respectively (Figure 6). The group of such different curves illustrates the existence of zone of metastable states in line width–temperature space. This means that varying the rate of sample cooling near the temperature of phase transition allows one to change the ordering degree of the octahedra in the sample. The presence of the entire metastable zone has not been observed before in the studies of oxyfluoride compounds.

The stability has been studied for some of the observed states at different temperatures. At fixed sample temperatures, the spectra were taken every 30 s during 4 to 7 h. The experimental data obtained below the phase transition at  $T = 10, 100,$  and 140 K and above phase transition at  $T = 205$  K are given in Table 2. As seen from Table 2, the line width in the cubic phase

**Table 2. Temperature Dependence of the Relaxation Rate**

temp (K)	relaxation rate ( $\text{cm}^{-1}/\text{h}$ )
205	$0.0013 \pm 0.0034$
140	$0.0152 \pm 0.0021$
100	$0.0082 \pm 0.0005$
10	$0.0039 \pm 0.0002$

at  $T = 205$  K remains constant, implying that this state is stable and there is no relaxation. Below the phase transition at  $T = 10$  K one can see that the line width changes with time for the sample state obtained by cooling at 10 K/min. We have measured the line width for 7 h and then made a linear approximation to estimate the relaxation rate. Using this value we estimated that it would take at least 7 days for the line width to decrease to the value typical for the 0.2 K/min cooling rate. The relaxation rate for the sample states at  $T = 205, 140, 100,$  and 10 K has been determined. Above  $T = 100$  K, the relaxation rate increases drastically, and at  $T = 140$  K, it is estimated to be  $0.015 \text{ cm}^{-1}/\text{h}$ . Still at helium temperatures, the lifetime of metastable states is measured in days.

The line width behavior during heating is found to be in complete agreement with the classical behavior.<sup>26</sup> After the initial heating, the line width plots obtained at different cooling rates are shifted with respect to each other (Figure 4a, Figure 7). Suppose the lowest temperature dependence on the line

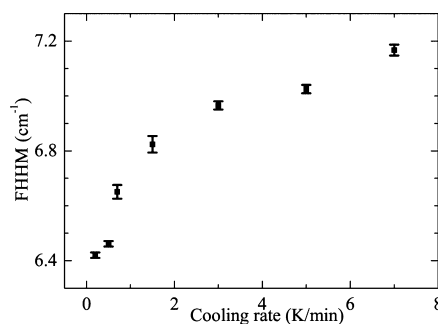


**Figure 7.** Linewidth of the Mo–O stretching vibration for different states obtained at different cooling rates and measured at  $T = 110$  K.

width, which is obtained in quasi-equilibrium conditions (cooling rate less than 0.2 K/min), to be an equilibrium one. The line width in this equilibrium state can be described by classical behavior up to the phase transition temperature. At the same time, the line width vs temperature dependence in each metastable state can be characterized by a critical temperature above which the behavior is no longer classical and the line width approaches the equilibrium value with time (Figure 6). The experiment with different heating rates has revealed that after passing a critical point, the line width remains almost constant until it reaches the equilibrium value. Critical points are about 90 K for the cooling rate 15 K/min and 140 K for the cooling rate of 10 K/min. In that way, we can estimate the biggest possible line width and it should be about  $8.5 \text{ cm}^{-1}$ . Based on the experimental data presented in Figure 7 at a cooling rate of 30 K/min, the line width vs temperature curve will be shifted away from the equilibrium curve by about  $1.6 \text{ cm}^{-1}$ , and the critical temperature is estimated to be about 10 K. A full possible width of the metastable zone could be obtained. The experimentally observed controllable area is denoted by double shading and the estimated area is indicated by single shading in Figure 6. Unfortunately, the cooling power of our cryostat does not make possible experiments with cooling rate more than 17 K/min in a controllable way; thus we were limited to use cooling rate in our experiments of not more 15 K/min.

We had investigated temperature phase transitions in oxyfluoride crystals before this experiment.<sup>17,27–31</sup> However, never before had we observed the effects discussed above.

In summary, the anomalous line width broadening of the fully symmetric vibrations of the anion octahedra in the crystal samples of  $\text{Rb}_2\text{KMoO}_3\text{F}_3$  elpasolite has been observed. It has been found that this line width broadening gives rise to an entire range of metastable states differing by disorder degree in the low temperature phase. It is possible to control the disorder degree of the octahedral groups by varying the cooling rate when passing through the point of phase transition. The anomalous line width, range of metastable states, and control over the degree of ordering are rarely seen in crystalline compounds. In addition, the current study demonstrates the advantage of the dynamic temperature regime for investigating ordering processes in crystals.

## ■ ASSOCIATED CONTENT

### Web-Enhanced Feature

A web-enhanced object in AVI format is available.



## ■ AUTHOR INFORMATION

## Corresponding Author

\*E-mail: shusy@iph.krasn.ru.

## Notes

The authors declare no competing financial interest.

## ■ ACKNOWLEDGMENTS

The authors are grateful to Prof. I. N. Flerov for valuable support and useful discussions. The authors acknowledge stimulating discussions with Dr. S. N. Sofronova and Dr. A. S. Aleksandrovsky. The assistance of Dr. S. Skokov is sincerely appreciated. This work was partly supported by Russian Foundation for Basic Research project nos. 11-02-98002-r and 12-02-00056 and integration project SB RAS no. 28, SS-4828.2012.2 grant, and Federal Special Program "Scientific and scientific-pedagogical staff of innovative Russia" (no. 8379).

## ■ REFERENCES

- (1) Dehnicke, Von K.; Pausewang, G.; Rüdorff, W. Z. *Anorg. Allg. Chem.* **1969**, 366 (1–2), 64–72.
- (2) Atuchin, V. V.; Gavrilova, T. A.; Isaenko, L. I.; Kesler, V. G.; Molokeyev, M. S.; Zhurkov, S. A. *Ceram. Int.* **2012**, 38, 2455–2459.
- (3) Udovenko, A. A.; Laptash, N. M. *Acta Crystallogr.* **2008**, B64, 305–311.
- (4) Welk, M. E.; Norguist, A. J.; Stern, C. L.; Poepplermier, K. R. *Inorg. Chem.* **2000**, 39, 3946–3947.
- (5) Sergienko, V. S.; Porai-Koshits, M. A.; Khodashova, T. S. *J. Struct. Chem.* **1972**, 13 (3), 431–436.
- (6) Maggard, P. A.; Kopf, A. L.; Stern, C. L.; Poepplermier, K. R. *Inorg. Chem.* **2002**, 41, 4852–4858.
- (7) Fokina, V. D.; Flerov, I. N.; Gorev, M. V.; Molokeyev, M. S.; Vasiliev, A. D.; Laptash, M. N. *Ferroelectrics* **2007**, 347, 60–64.
- (8) Withers, R. L.; Welberry, T. R.; Brinc, F. J.; Noren, L. *Solid State Chem.* **2003**, 170, 211–220.
- (9) Pogoreltsev, E. I.; Bogdanov, E. V.; Molokeyev, M. S.; Voronov, V. N.; Isaenko, L. I.; Zhurkov, S. A.; Laptash, N. M.; Gorev, M. V.; Flerov, I. N. *Phys. Solid State* **2011**, 53 (6), 1202–1211.
- (10) Peraudeau, G.; Ravez, J.; Haggemuller, P.; Arend, H. *Solid State Commun.* **1978**, 27, 591–593.
- (11) Abrahams, S. C.; Bernstein, J. L.; Ravez, J. *Acta Crystallogr.* **1981**, B37, 1332–1336.
- (12) Ravez, J.; Peraudeau, G.; Arend, H.; Abrahams, S. C.; Haggemuller, P. *Ferroelectrics* **1980**, 26, 767–769.
- (13) Peraudeau, G.; Ravez, J.; Arend, H. *Solid State Commun.* **1978**, 27, 515–518.
- (14) Couzi, M.; Rodriguez, V.; Chaminade, J. P.; Fouad, M.; Ravez, J. *Ferroelectrics* **1988**, 80, 109–112.
- (15) Krylov, A. S.; Merkusheva, E. M.; Vtyurin, A. N.; Isaenko, L. I. *Phys. Solid State* **2012**, 54 (6), 1275–1280.
- (16) D. A. Long *The Raman Effect*; J. Wiley & Sons, Ltd: New York, 2002.
- (17) Krylov, A. S.; Gerasimova, Yu. G.; Vtyurin, A. N.; Fokina, V. D.; Laptash, N. M.; Voit, E. I. *Phys. Solid State* **2006**, 48 (7), 1356–1362.
- (18) Malinovsky, V. K.; Pugachev, A. M.; Surovtsev, N. V. *Phys. Solid State* **2008**, 50 (6), 1137–1143.
- (19) Baldinozzi, G.; Ph. Sciau; Bulou, A. *J. Phys.: Condens. Matter* **1997**, 9, 10531–10544.
- (20) Krylova, S. N.; Vtyurin, A. N.; Bulou, A.; Krylov, A. S.; Zamkova, N. G. *Phys. Solid State* **2004**, 46 (7), 1311–1319.
- (21) Krylov, A. S.; Krylova, S. N.; Vtyurin, A. N.; Surovtsev, N. V.; Adishev, S. V.; Voronov, V. N.; Oreshonkov, A. S. *Crystallogr. Rep.* **2011**, 56 (1), 18–23.
- (22) Ouilon, R.; Turc, C.; Lemaistre, J.-P.; Ranson, P. *J. Chem. Phys.* **1990**, 93, 3005–3011.
- (23) Clouter, M. J.; Kieft, H.; Jain, R. K. *J. Chem. Phys.* **1980**, 73, 673–682.
- (24) Hwang, C.; Fleury, P. A. *Light Scattering Spectra of Solids*; Wright, G. B., Ed.; Springer-Verlag: New York, 1969; pp 651–663.
- (25) Musso, M.; Matthai, F.; Keutel, D.; Oehme, K. *J. Chem. Phys.* **2002**, 116 (18), 8015–8027.
- (26) Ramkumar, C.; Jain, K. P.; Abbi, S. C. *Phys. Rev. B* **1996**, 53, 13672–13681.
- (27) Fokina, V. D.; Flerov, I. N.; Molokeyev, M. S.; Pogoreltsev, E. I.; Bogdanov, E. V.; Krylov, A. S.; Bovina, A. F.; Voronov, V. N.; Laptash, N. M. *Phys. Solid State* **2008**, 50 (11), 2175–2183.
- (28) Krylov, A. S.; Goryainov, S. V.; Vtyurin, A. N.; Krylova, S. N.; Sofronova, S. N.; Laptash, N. M.; Emelina, T. B.; Voronov, V. N.; Babushkin, S. V. *J. Raman Spectrosc.* **2012**, 43, 577–582.
- (29) Krylov, A. S.; Krylova, S. N.; Vtyurin, A. N.; Laptash, N. M.; Kocharova, A. G. *Ferroelectrics* **2012**, 430, 65–70.
- (30) Ekimov, A. A.; Krylov, A. S.; Vtyurin, A. N.; Ivanenko, A. A.; Shestakov, N. P.; Kocharova, A. G. *Ferroelectrics* **2010**, 410, 168–173.
- (31) Mel'nikova, S. V.; Krylov, A. S.; Zhogal', A. L.; Laptash, N. M. *Phys. Solid State* **2009**, 58 (4), 817–822.